



The global atmospheric energy transport analysed by a wavelength-based scale separation

Patrick Johannes Stoll¹ and Rune Grand Graversen^{1,2}

¹Department of Physics and Technology, Arctic University of Norway, Tromsø, Norway

²Norwegian Meteorological Institute, Norway

Correspondence: Patrick Johannes Stoll (patrick.stoll@uit.no)

Abstract.

The global atmospheric circulation is fundamental for the local weather and climate by redistributing energy and moisture. To the present day, there is a knowledge gap at which spatial scales the energy and its components are transported. Therefore, we separate the meridional atmospheric energy transport in the ERA5 reanalysis by the spatial scales, the quasi-stationary and transient flow patterns, and the latent and dry-static component. We focus on the annual and seasonal mean in the transport components as well as their inter-annual variability. Motivated by similarities across latitudes in the atmospheric transport spectra when displayed as function of wavelength, we refine the existing scale separation method to be based on wavelength instead of wavenumber.

This reveals advantageous, as the following conclusions can be drawn, which are fairly similar in the two hemispheres. Transport by synoptic waves, defined at wavelengths between 2,000 and 8,000 km, is the largest contributor to extra-tropical energy and moisture transport, is mainly of transient character, and is little influenced by seasonality. In contrast, the transport by planetary waves, larger than 8,000 km, highly depends on the season and has two distinct characteristics. (1) In the extra-tropical winter, planetary waves are of major importance due to transport of dry-static energy. This planetary transport feature the largest inter-annual variability, and is mainly quasi-stationary in the Northern Hemisphere, but transient in its southern counterpart. (2) In the subtropical summer, quasi-stationary planetary waves are the most important transport component mainly due to advection of moisture, which is associated with monsoons. In contrast to transport by planetary and synoptic waves, only a negligible amount of energy is transported by mesoscale eddies ($< 2,000$ km).

1 Introduction

The atmosphere is in motion to reduce the thermal contrast created by differential solar heating between high and low latitudes (Hadley, 1735). Hence the atmospheric circulation transports energy polewards (Oort and Peixoto, 1983), and has hereby a fundamental role for the local weather and climate (e.g. Holton and Hakim, 2013; Vallis, 2017). The energy is primarily transported in form of warm air (dry-static: comprising mainly enthalpy and potential energy), and water vapour (latent energy) which releases energy when condensating before precipitation (Peixoto and Oort, 1992).



The manner the atmosphere is transporting energy is different among climate zones (Trenberth and Stepaniak, 2003a). In the tropics and sub-tropics, where the Coriolis effect is small, energy is predominantly transported by a meridional overturning circulation, the Hadley cell and monsoon systems (Hadley, 1735) (Fig. 1). In the extra-tropics, eddies take over to transport the energy further poleward. Atmospheric eddies exist on a large range of scales, from planetary and synoptic Rossby waves (Rossby, 1939), via synoptic cyclones (Bjerknes, 1919), to mesoscale disturbances, such as polar lows (Businger and Reed, 1989). Traditionally, the eddy transport is separated into a quasi-stationary and a transient component (Fig. 1a), with the former representing monthly-mean eddies and the latter fast-varying deviations from this mean (Oort and Peixóto, 1983). Here we revise the traditional separation and compare it to a partition based on the spatial scale.

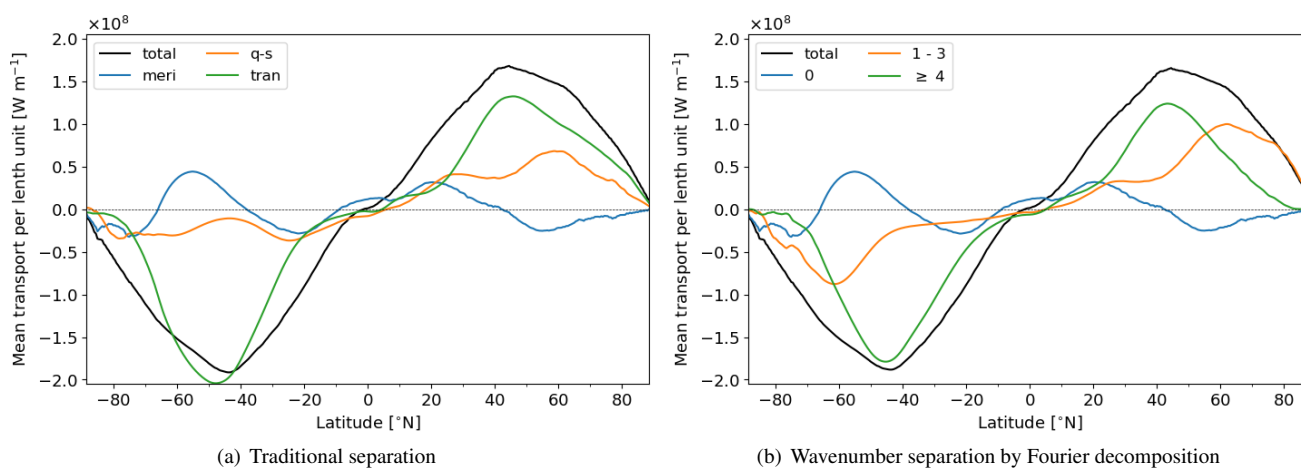


Figure 1. Different separation methods of the vertical-integrated, zonal-mean, northward transport of energy from ERA5 as mean of the years 1979 to 2018. (a) The traditional partition into the meridional overturning circulation (meri), quasi-stationary (q-s), and transient (tran) eddies, as performed by Oort and Peixóto (1983). (b) A decomposition into transport by different spatial scales defined by wavenumbers as suggested by Graversen and Burtu (2016). Transport by wave 0 provides the meridional overturning circulation. The sum of transport by waves 1 - 3 is often associated with planetary transport, whereas waves with larger wavenumbers are considered to be of synoptic scale.

Recent studies demonstrate the usefulness of separating the energy transport into planetary and synoptic-scale components, as for instance, these two types of waves impact the Arctic differently (Baggett and Lee, 2015; Graversen and Burtu, 2016). The scale separation of the energy transport by Fourier decomposition became popular in recent years as it was applied to study the effect of energy transport for the Arctic (Papritz and Dunn-Sigouin, 2020; Graversen et al., 2021; Rydsaa et al., 2021; Hofsteenge et al., 2022), and for the mid-latitudes of the Northern Hemisphere (NH) (Lembo et al., 2019; Röthlisberger et al., 2019; Vihma et al., 2020). These studies separate the transport by a wavenumber which is independent of the latitude as depicted in Figure 1b. However, the wavelength associated with a given wavenumber is latitude dependent (Fig. 2). Therefore the partitioning by wavenumber, for example between wave 3 and 4 as performed in many of the previously mentioned studies, leads to convergence of all eddy transport to the planetary scale towards the poles, whereas synoptic transport may be overestimated at low latitudes (Fig. 1b). Wave 4 for instance corresponds to a wavelength of 8200 km at 35°, but only to 2600 km at



75°, which can be interpreted to represent different spatial scales. Accordingly, Heiskanen et al. (2020) recommend to consider the threshold for separation between two wavenumbers with care.

To circumvent this problem occurring with separation by wavenumber, we refine the scale separation method by Graversen and Burtu (2016) to be based on the wavelength instead. Hereby, we partition the transport into planetary, synoptic and mesoscale components to further improve our understanding of the global atmospheric circulation. In addition, we apply the established decomposition of the energy transport into stationary and transient parts (Fig. 1a), as well as dry-static and latent components (Peixoto and Oort, 1992).

The new scale-separation method is employed to analyse the global atmospheric circulation. Previous studies found that transport by quasi-stationary waves is important in the Northern Hemisphere (NH), but almost negligible in the Southern Hemisphere (SH) (e.g. Peixoto and Oort, 1992). Such quasi-stationary transport is often associated with the planetary scale, which appears to imply that planetary transport is irrelevant in the SH (e.g. Trenberth and Stepaniak, 2003a). In contrast, transport by transient eddies is often associated with baroclinic eddies at the synoptic scale (e.g. Trenberth and Stepaniak, 2003a). However, transport at other scales could be of transient character as well. In this study, we are pointing out that the separation of transport into a quasi-stationary and transient contribution is different from a separation into planetary and synoptic scales. Although a correlation exists between the two especially for the NH.

To summarise the main research questions posed in this study:

1. At what scales does the atmosphere transport energy?
2. How does the traditional separation method compares to the scale separation method?
3. What characterises the atmospheric energy transport in different climate zones?

However, first the utilised data and methods are presented.

2 Data and methods

2.1 ERA5 reanalysis

The atmospheric energy transport from the period 1979 - 2021 is analysed with ERA5 (Hersbach et al., 2020), the fifth atmospheric reanalysis from the European Centre for Medium-Range Weather Forecasts (ECMWF), which substituted its precursor ERA-I in 2019. ERA5 provides hourly fields at a spectral truncation of T639, which is equivalent to a grid spacing of 30 km with 137 vertical hybrid levels. For this study, fields of temperature, humidity, geopotential height and horizontal wind components at all hybrid levels, and surface pressure and surface topography are used at a $0.25^\circ \times 0.25^\circ$ horizontal grid spacing. Since reanalysis data are prone to include mass-flux inconsistencies (Trenberth, 1991), a barotropic mass-flux correction is applied to the wind field prior to calculating the energy transport (Graversen, 2006).

In this study, we take a zonal-mean perspective of the atmospheric energy transport, which provides the transport through an atmospheric column with one metre width. Hereby, it provides a local measure of the transport, and differs from other studies



that zonally integrate the transport along each longitude circle (Peixoto and Oort, 1992; Trenberth and Caron, 2001; Graversen and Burtu, 2016). However, the computed zonal integral of the energy transport from ERA5 (Fig. S1a) confirms the transport
 75 in these studies. For instance, the zonal-integrated poleward transport peaks at 4.8×10^{15} W in the NH and 5.6×10^{15} W in the SH at 41° latitude in both hemispheres. The latitude of maximum zonal-mean transport is slightly higher at 45° (Fig. S1b). Further, the average transport in the polar regions is more easily assessed by the zonal-mean transport as it is not influenced by converging latitudes.

The zonal-mean energy transport is smoothed with a 2° running-mean filter along the meridional dimension for noise re-
 80 duction. For the calculation of convergence of energy transport this filter is used before and after computing the meridional derivatives.

2.2 Decomposition of the energy transport

The atmospheric energy transport and its components are characterised by a large day-to-day variability (Lembo et al., 2019). However, we take a annual-mean and season-mean perspective of the energy transport, since one purpose of this study is the
 85 comparison of the traditional separation of the transport by quasi-stationary and transient eddies with a separation based on spatial scales. This comparison is only possible from a time-mean perspective, since the quasi-stationary transport is normally derived based on monthly-mean fields (Oort and Peixoto, 1983). A subsequent study is planned for investigating the short time variability of the different energy transport components.

This study investigates the vertically-integrated, zonal-mean, time-mean, meridional transport of atmospheric energy,

$$90 \quad \widetilde{vE} = \int_0^{p_s} [\overline{vE}] \frac{dp}{g}, \quad (1)$$

where $\mathbf{v} = (u, v)$ are the zonal and meridional wind components, E an energy component, p pressure, p_s surface pressure, g gravitational constant, $\overline{\cdot}$ denoting a monthly time average, and $[\cdot]$ the zonal average. We decompose the total atmospheric energy transport, \widetilde{vE} , in three ways that can be applied in combination:

1) Into latent energy transport \widetilde{vQ} , and dry-static energy transport \widetilde{vD} . This is achieved by separating the energy into its
 95 latent component, Q , and dry-static component, D , comprising the enthalpy, $C_p T$, potential energy, gz , and kinetic energy, $\frac{\mathbf{v}^2}{2}$,

$$E = Q + D = Lq + \left(C_p T + gz + \frac{\mathbf{v}^2}{2} \right), \quad (2)$$

with q being specific humidity, L the latent heat release by condensation, C_p specific heat capacity at constant pressure, and T temperature.

2) Into monthly-mean transport by transient eddies, \widetilde{vE}^{tran} , quasi-stationary eddies, \widetilde{vE}^{q-s} , and the mean meridional cir-
 100 culation, \widetilde{vE}^{meri} , derived by the following equation according to Peixoto and Oort (1992),

$$[\overline{vE}] = [\overline{v'E'}] + [\overline{v^*E^*}] + [\overline{v}][\overline{E}], \quad (3)$$



with \cdot' anomalies from the time mean, and \cdot^* stating zonal anomalies from the zonal mean. Hereby, the quasi-stationary transport provides the transport given by the monthly-mean fields, and the transient transport is the residual fast varying component. The annual-mean energy transport partitioned in this traditional manner is depicted in Figure 1a.

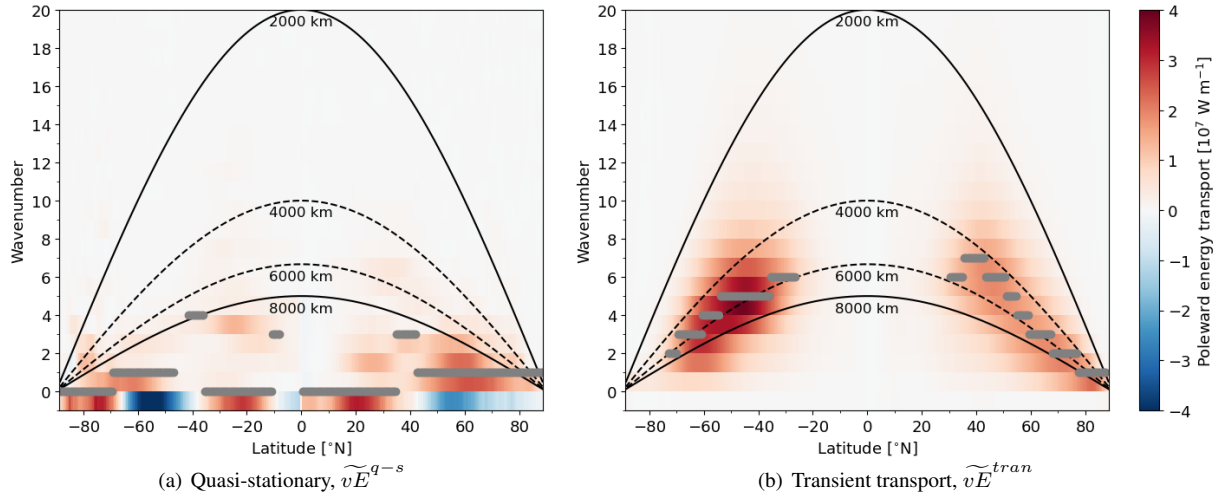


Figure 2. The annual-mean, zonal-mean of the Fourier-decomposed poleward transport of energy from ERA5 for each latitude. (a) Depicts the decomposition of the quasi-stationary and (b) of the transient energy transport. The wavenumbers corresponding to some wavelengths are presented by black curves. The solid curves at 2,000 and 8,000 km denote the separation between meso, synoptic and planetary scale. At each latitude the wave of maximal poleward energy transport is denoted in grey, where values are masked if the wave is responsible for less than 5% of the transport at the latitude with maximum transport.

105 3) Into planetary-scale transport, \widetilde{vE}_{plan} , synoptic-scale transport, \widetilde{vE}_{syno} , mesoscale transport, \widetilde{vE}_{meso} , and the meridional circulation, \widetilde{vE}_{meri} . For the partition into spatial scales the Fourier decomposition is applied along each latitude, ϕ , and at each vertical model level at every time step following Graversen and Burtu (2016),

$$E = \frac{a_0^E}{2} + \sum_{n=1}^{\infty} a_n^E \cos\left(\frac{n2\pi x}{d}\right) + b_n^E \sin\left(\frac{n2\pi x}{d}\right), \quad (4)$$

with x the zonal coordinate, $d = 2\pi a \cos(\phi)$, $a = 6371$ km Earth's radius, and the coefficients:

$$110 \quad a_n^E = \frac{2}{d} \oint E \cos\left(\frac{n2\pi x}{d}\right) dx, \quad b_n^E = \frac{2}{d} \oint E \sin\left(\frac{n2\pi x}{d}\right) dx. \quad (5)$$

In a similar manner coefficients are derived for the meridional wind, v : a_n^v and b_n^v . The transport associated with the meridional circulation is then given by:

$$[vE]_{meri} = \frac{1}{4} a_0^v a_0^E. \quad (6)$$

which becomes similar to \widetilde{vE}^{meri} for monthly time averages.



115 The zonal-mean transport by wave n is becoming

$$[vE]_n = \frac{1}{2} (a_n^v a_n^E + b_n^v b_n^E). \quad (7)$$

The transport by each wave as function of latitude is displayed in Figure 2 for the quasi-stationary and transient transport component.

To separate the energy transport between the scale s and the next smaller scale $s + 1$ at larger wavenumber, the latitudinal-
 120 dependent (ϕ) separation number, n_{s+1} , is computed based on the predefined wavelength, λ_{s+1} :

$$n_{s+1} = \frac{2\pi \cdot a \cdot \cos(\phi)}{\lambda_{s+1}}. \quad (8)$$

To separate planetary waves from the meridional overturning circulation, $n_{plan} = 0$ is applied. For the separation between plan-
 etary and synoptic waves, the separation number, n_{syno} , is computed at each latitude from the wavelength $\lambda_{syno} = 8,000$ km
 (lower black solid line in Fig. 2). Synoptic and mesoscale eddies are separated at a wavelength of $\lambda_{meso} = 2,000$ km. In Sec-
 125 tion 3, we argue for the usage of these two wavelengths for scale-separating the energy transport. The separation numbers
 as defined here are real numbers. To ensure a continuous separation (Fig. S2a), instead of abrupt transitions (Fig. S2b), the
 transport given by eddies of spatial scale, s , is defined by:

$$[vE]_s = ([n_s] - n_s) \cdot [vE]_{[n_s]} + \sum_{n=[n_s]+1}^{[n_{s+1}]} [vE]_n + (n_{s+1} - [n_{s+1}]) \cdot [vE]_{[n_{s+1}]}, \quad (9)$$

with $[\cdot]$ rounds to the integer part and $\lceil \cdot \rceil$ rounds to the least integer. Equation 9 provides the separation depicted in Figure 2
 130 between the black solid lines representing the separation numbers. An underlying interpretation is that at a latitude circle of
 for instance 30,000 km, wave 1 includes the energy at a scale larger than 15,000 km, wave 2 of between this and 10,000 km
 and so forth. Spectra depicting the separation into the scale components at different latitudes are provided in Figure S3 and an
 example for the separation is provided in Supplement Section 3.

3 Wavelengths utilised for scale separation

135 Orlanski (1975) defines the mesoscale to be smaller than 2,000 km, which is commonly accepted and hence utilised as threshold
 in this study for separation towards the larger synoptic scale. However, a widely-agreed separation between the planetary and
 synoptic scale has not been established. For the following reasons we implement the separation between the planetary and
 synoptic scale at a wavelength of 8,000 km, even though the exact value is to some degree arbitrary:

1) The synoptic scale is supposed to include most energy transport associated with synoptic cyclones developing by baro-
 140 clinic instability (Vallis, 2017; Holton and Hakim, 2013). The scale (wavelength) of baroclinic eddies is estimated to be
 4,000 km by (Vallis, 2017, p.354) and 4,800 km by Stoll et al. (2021). Note, that a low-pressure system spans half a wave-
 length, and has accordingly a typical size of around 2,000 km. Since synoptic cyclones feature some variability in their size,
 and in the Fourier decomposition considerable amount of the energy transport is occurring on neighbouring waves (Heiskanen
 et al., 2020, Fig. 3), a wavelength band between 2,000 - 8,000 km appears appropriate to capture the majority of the transport



145 associated with synoptic cyclones. However, this band also includes transient synoptic Rossby waves (e.g. Röthlisberger et al.,
2019; Ali et al., 2021) which may interact with cyclones in a baroclinic manner. Also other processes than baroclinic instabil-
ity, likely contribute to the formation of the here-defined synoptic eddies, such as heating contrasts. A future study is going to
investigate the causes for eddy transport at different scales.

2) Previous studies performing a wave decomposition qualitatively agree on the separation at a wavelength of 8,000 km:

150 2a) Baggett and Lee (2015) perform a Fourier decomposition of energy characteristics for the entire NH and demonstrate
different life cycle behaviour of long (planetary) and short (synoptic) waves for a separation between wave 3 and 4. Ali et al.
(2021) identifies recurrent synoptic-scale transient Rossby wave packets in the mid-latitudes at wavenumbers between 4 and
15. Their separation into planetary and synoptic eddies between waves 3 and 4 is similar to the here-applied partitioning at a
wavelength of 8,000 km at 53° latitude which is close to the zone of maximum eddy activity (Fig. 1). For a hemisphere-wide
155 separation into planetary and synoptic eddies with one wavenumber of separation as utilised by Baggett and Lee (2015) and
Ali et al. (2021), it appears crucial to capture the partition around this zone.

2b) At 70° N, a wavelength of 8,000 km is associated with a separation number $n_{syno} = 1.7$, meaning that 70% of wave 2 is
associated with the planetary scale and 30% to the synoptic scale. Accordingly, the lead-lag regression of the Arctic temperature
to the latent transport presented in Fig. 6 of Graversen and Burtu (2016) shows a clear difference between wave 1, leading to
160 heating of the Arctic, and waves 3 and larger, having a baroclinic signal. Wave 2 appears to share characteristics between the
wave 1 and waves larger than 2, in agreement with the here applied separation number that divides wave 2. Also Heiskanen
et al. (2020) find a good attribution of an idealised cyclone to the synoptic scale, if the separation between the planetary and
synoptic scale is performed at rather small wavenumbers even though they do not test a separation between wave 2 and 3.

3) The partition at a wavelength of 8,000 km approximately captures our intuitive understanding that synoptic cyclones and
165 synoptic Rossby wave packets are transient by nature, whereas planetary waves are more quasi-stationary, since they may be
constraint by locally-fixed orography and large-scale and semi-stationary thermal forcing, such as heating contrasts between
ocean and land (Vallis, 2017), as we show in the following:

The spectral decomposition of the annual-mean energy transport, \widetilde{vE} , at different latitudes reveals that most eddies smaller
than 8,000 km are of transient nature, whereas most of the quasi-stationary transport is at scales larger than 8,000 km (Fig. 2).
170 For the transient energy transport, the wavenumber of maximum transport is 6 or 7 in the subtropics and decreases towards the
poles, such that the corresponding wavelength of maximum transient transport is around 5,000 to 6,000 km for all latitudes.
Also in the moisture transport, the transient component reaches its maximum around 5000 km (Fig. S4), which is in good
agreement with Lee et al. (2019). This wavelength corresponds well to the preferred scale of baroclinic eddies (4,000 - 5,000 km
Vallis, 2017; Stoll et al., 2021). The independence of the scale of maximum transient transport from latitudes provides a major
175 argument that the separation between the synoptic and planetary scale is better achieved by a threshold based on wavelength
rather than wavenumber when the transport across all latitudes is examined.

It may appear surprising that the scale of maximum transient energy transport, \widetilde{vE}^{tran} , is independent of the latitudes,
since the deformation radius estimating the size of baroclinic eddies depends inversely on the Coriolis parameter, and depends
linearly on the layer depth which decreases with latitude (Vallis, 2017). However, these are parameters important for the



180 cyclogenesis which is mostly active in a confined region: Most cyclones originate from the mid-latitudes, where the horizontal temperature contrast is largest. The size of a cyclone is set during the genesis stage when the fastest-growing mode is prevailing. Many cyclones propagate to higher latitudes along the diagonal axis of the storm tracks (Shaw et al., 2016) and may keep their size.

The preferred wavenumber and wavelength of the quasi-stationary transport, \widetilde{vE}^{q-s} , are latitude dependent (Fig. 2a). The wavenumber of maximum quasi-stationary transport is larger than 8,000 km everywhere besides close to the North Pole where the Fourier decomposition is not applicable and around 40° S where the quasi-stationary transport is almost negligible. A short analysis of the preferred scales of the quasi-stationary transport is provided in Supplement 4.

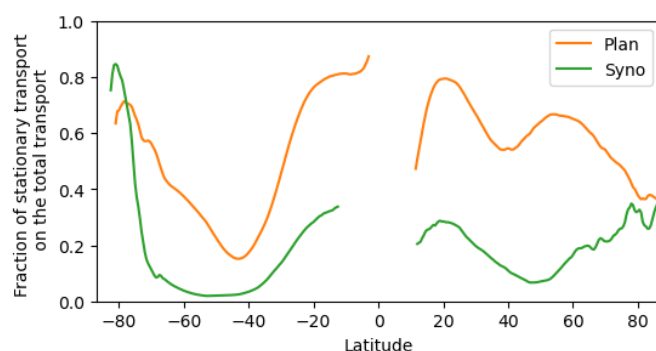


Figure 3. The fraction of the quasi-stationary part of the transport by planetary and synoptic waves as a function of latitude from ERA5.

Based on the partitioning into transient and quasi-stationary eddies, we here argue for the wavelength of 8,000 km for separating between synoptic and planetary waves. However, it is evident that the traditional decomposition of the transport into stationary and transient parts (Oort and Peixóto, 1983) is not equivalent to a separation into planetary and synoptic waves: Planetary waves at a wavelength larger than 8,000 km can be both transient and quasi-stationary (Fig. 2). In the latitude band between 70 and 30° S and poleward of 70° N, zones mainly characterised by open ocean, the transient component within the planetary transport is larger than the quasi-stationary component (Fig. 3). At latitudes with more land, the quasi-stationary component is responsible for 50 - 80% of the planetary transport, meaning that also at these latitudes a considerable proportion of the planetary transport is transient. Also the moisture transport, \widetilde{vQ} , comprises a planetary component that features transient and quasi-stationary characteristics similar to the total energy transport, \widetilde{vE} (Fig. S5).

In contrast, the synoptic transport is mainly (70 - 100%) of transient nature at all latitudes, which coincides with the transient character of synoptic cyclones and Rossby waves of short wave length. Hence in the following, the quasi-stationary component of synoptic transport is not further investigated. An exception for the transient character of synoptic transport is over Antarctica, which is characterised by katabatic flows advecting cold air towards lower latitudes, occurring at preferred locations of drainage, hence including a large stationary component.

In conclusion, a separation at 8,000 km appears to capture our intuitive understanding of the planetary and synoptic scales. However, as mentioned earlier, a clear threshold likely does not exist. Therefore, the separation wavelength of 8,000 km is



Table 1. The applied climate zones in this study.

Climate zone	Latitude band
Equatorial region	$< 10^\circ$
Tropics	$< 23^\circ$
Sub-tropics	$23^\circ - 35^\circ$
Extra-tropics	$35^\circ - 90^\circ$
Mid-latitudes	$35^\circ - 60^\circ$
Polar boundary	Around 60°
Polar regions	$60^\circ - 90^\circ$

compared to wavelengths of 10,000 km and 6,000 km in the Supplement (Fig. S6). The main results of this study are not
205 affected by the exact choice of the separation wavelength.

4 Organisation of the global energy transport

In this section, we analyse the atmospheric energy transport from ERA5 by utilising the scale-separation method. The applied climate zones used in this study are provided in Table 1.

4.1 Annual-mean transport

210 Overview

The meridional atmospheric energy transport features large similarities for the two hemispheres in most components for most climate zones (Fig. S6) and to simplify the comparison of the two hemispheres, we display the poleward transport of both hemispheres on a common axis (Fig. 4).

The annual-mean, zonal-mean poleward energy transport, \widetilde{vE} , is seamless in the sense that it resembles half of a sine curve
215 for both hemispheres (black lines in Fig. 4a) as noted by Trenberth and Stepaniak (2003b). The poleward atmospheric energy transport is almost similar in both hemispheres, however, 15% larger in the subtropics and mid-latitudes of the SH than the NH, largely balanced by more oceanic transport in the NH (Trenberth and Caron, 2001).

The energy transport, \widetilde{vE} , causes annual-mean divergence of around 40 W m^{-2} in the tropics and subtropics and convergence at latitudes poleward of 40° latitude of up to 100 W m^{-2} in the polar regions (Fig. 4d) in good agreement with Trenberth and
220 Stepaniak (2003a). The smaller divergence close to the equator is due to oceanic currents transporting heat to the subtropics and hence creating a cold tongue of sea-surface temperatures over the equatorial Pacific (Trenberth and Stepaniak, 2003b).

Despite the total energy transport, \widetilde{vE} , appearing seamless, different transport mechanisms are important in the climate zones expressed by a considerable variations across latitudes in the moisture and dry-static transport (Fig. 4b and c), and in the scale components of the transport.

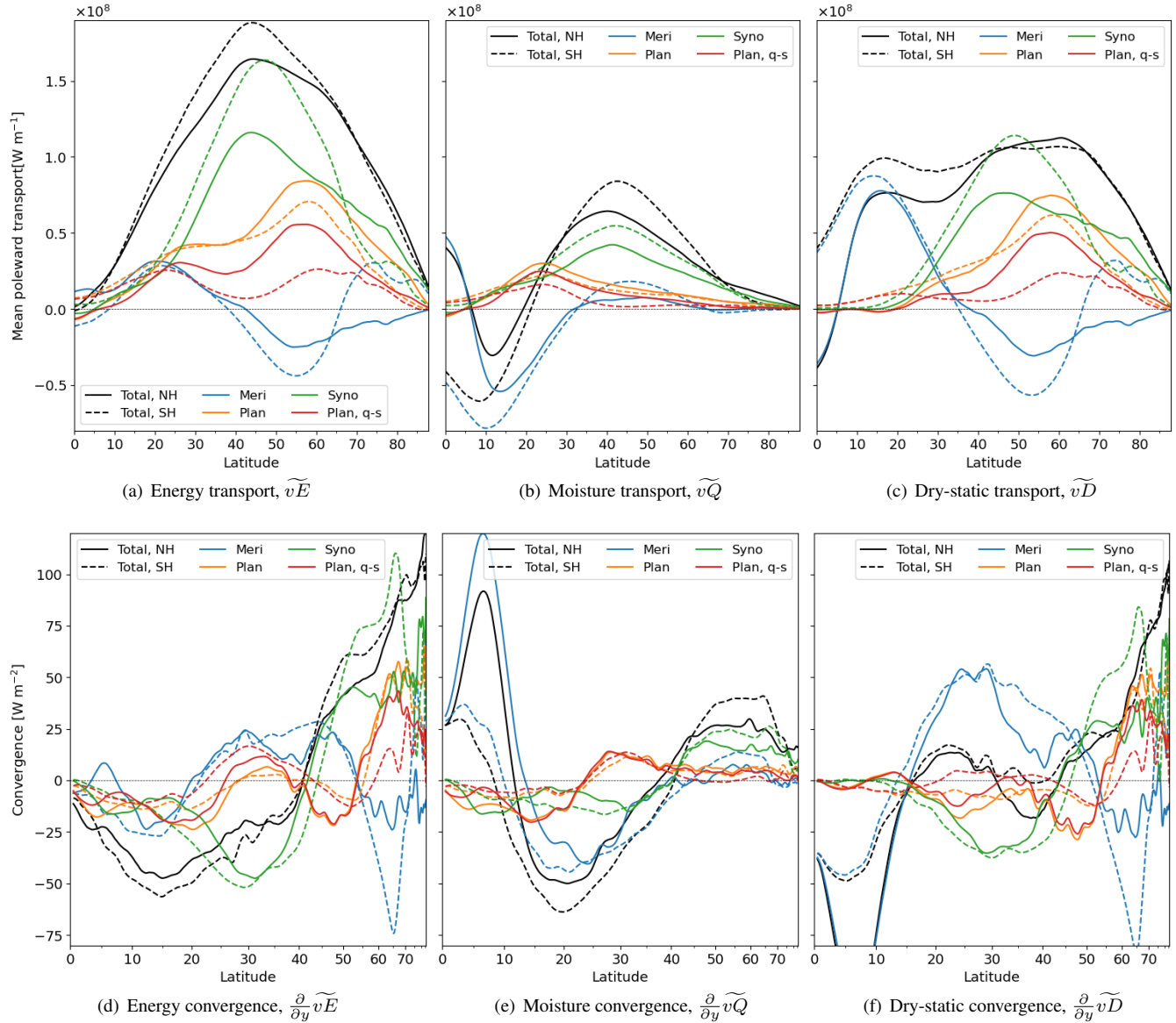


Figure 4. (a) Annual-mean, zonal-mean poleward atmospheric energy transport from ERA5 for the years 1979 - 2021. The transport of the Northern and Southern Hemisphere are depicted in solid and dashed lines, respectively. The total energy transport (black) is divided into the zonally symmetric meridional overturning circulation (blue) and wave components at the planetary (orange, waves $> 8,000$ km) and synoptic scale (green, $< 8,000$ km). The quasi-stationary contribution of the planetary transport on a monthly scale is depicted in red. (b) and (c) as (a) but for the latent and dry-static energy transport components, respectively. (d) - (f) Resulting convergence of atmospheric energy from the transport components presented in (a) - (c), with exception of the quasi-stationary planetary transport. The latitudes on the x-axis are scaled to represent equal surface areas.



225 To a first order, the annual-mean moisture transport, \widetilde{vQ} , resembles the inverse of a sine curve in each hemisphere with an exponentially decaying tail towards the poles (Fig. 4b). Hence, moisture transport in the tropics is equatorward and poleward in the subtropics and extra-tropics with a maximum around 40° latitude. This leads to moisture divergence in the non-equatorial tropics and sub-tropics and convergence in the equatorial regions and extra-tropics (Fig. 4e). The dry-static transport, \widetilde{vD} , features a plateau between 10-65° latitude (Fig. 4c). Hence, it is mainly responsible for divergence in the equatorial regions and convergence in the polar regions (Fig. 4f). However, the scale components have different roles in the climate zones.

230

Synoptic transport

Synoptic-scale waves are dominant in the transport of energy in the mid-latitudes of both hemispheres (Fig. 4a). Although synoptic transport is around 40% stronger in the SH than the NH. This is in broad agreement with the finding of Peixoto and Oort (1992) that transient transport is more relevant in the SH, but keeping in mind that some of the transient transport occurs at the planetary scale (Fig. 3). Despite a broad spectrum of possible waves, most energy is transported in the synoptic scale at wavelengths between 2,000 and 8,000 km, demonstrating the dominant role of synoptic waves for the mid-latitude energy transport (Fig. S6). This is different from previous studies that find that transient eddies are responsible for the majority of mid-latitude energy transport, since planetary waves may also be transient. The peak transport of synoptic waves is at around 45° latitude, the location of the climatological storm tracks (Priestley and Catto, 2022), and coincides with the zone of largest total energy transport. Hence, synoptic waves advect energy from the subtropics (< 40°) to the extra-tropics (Fig. 4d).

235

240

Extra-tropical synoptic waves transport approximately two thirds of their energy in dry-static form and one third in latent form, with the latent contribution being a bit more important in the low mid-latitudes and less important in the polar regions (Fig. 4b,c). Synoptic eddies are responsible for the majority of the extra-tropical moisture transport. Especially in the polar regions almost all moisture transport is by synoptic waves, whereas dry-static transport in the polar regions occurs at both synoptic and planetary scales.

245

Planetary transport

The planetary energy transport is almost similar in both hemispheres, different from the quasi-stationary transport that is mainly relevant in the NH (Fig. 4a). The planetary transport is similar in the subtropics and low mid-latitudes and only approximately 20% weaker in the higher mid-latitudes of the SH than the NH. This is in contrast to the previous interpretation that planetary transport being represented by the quasi-stationary component is mainly relevant in the NH (e.g. Trenberth and Stepaniak, 2003a). This is the case since the planetary transport has a highly relevant transient component in the SH (Fig. 3).

250

Generally two patterns of planetary transport are identified: 1) In the sub-tropics, most planetary transport is associated with quasi-stationary moisture transport, $\widetilde{vQ}_{plan}^{q-s}$. These waves represent subtropical high-pressure and monsoon systems, which can prevail for several weeks. The planetary moisture transport leads to humidity divergence in the tropics and convergences in the sub- and extra-tropics (Fig. 4e).

255

2) In the extra-tropics, planetary eddies mainly transport dry-static energy and only little moisture. In the polar regions, this planetary energy transport is almost as important as synoptic transport. The peak in energy transport by planetary waves,



\widetilde{vE}_{plan} , is at the polar boundary around 60° latitude in both hemispheres (Fig. 4a,c), hence further poleward to the peak in synoptic transport. Hence the planetary dry-static transport, \widetilde{vD}_{plan} , leads to energy divergence in the sub-tropics and mid-260 latitudes and convergence in the polar regions (Fig. 4f). The most remarkable difference between the hemispheres is that planetary waves are transient in the extra-tropical SH, whereas often quasi-stationary in its northern counterpart, which agrees with Peixoto and Oort (1992).

Meridional overturning circulation

The meridional overturning circulation, \widetilde{vE}_{meri} , and its role in transporting energy poleward have long been known (e.g. 265 Hadley, 1735; Lorenz, 1967; Peixoto and Oort, 1992). It constitutes the Hadley circulation in the tropics, which is dominating the energy transport in that region. The annual-mean total energy transport, \widetilde{vE}_{meri} , by the Hadley circulation is small compared to the latent, \widetilde{vQ}_{meri} , and dry-static components, \widetilde{vD}_{meri} , due to compensation between these two components (Fig. 4), and due to a compensation between the summer and winter season (see section 4.2). The meridional circulation, \widetilde{vE}_{meri} , features the thermally-indirect Ferrel cell in the mid-latitudes with a peak around 53°, which is almost twice as strong in the SH 270 than NH. The transport by the Ferrel cell is mainly in form of dry-static energy which is to a small amount compensated by moisture transport being thermally direct. In the NH, the Ferrel cell spans the whole extra-tropics including the Arctic. In the SH, a thermally-direct polar cell is evident in the dry-static transport, \widetilde{vD}_{meri} , which is primarily driven by katabatic flow from Antarctica as noted by Trenberth and Stepaniak (2003a).

Mesoscale transport

275 In contrast to synoptic and planetary waves, mesoscale waves, \widetilde{vE}_{meso} , at scales smaller than 2,000 km, are only responsible for a negligible part of the energy and moisture transport at all latitudes (Fig. 2, S6), well in accordance with Graversen and Burtu (2016), who show that wavenumbers 0-10 are responsible for almost all of the energy transport at all latitudes. Atmospheric models may have larger challenges to reproduce mesoscale eddies as compared to eddies at larger scales. However, ERA5 at a horizontal grid spacing of ≈ 30 km is able to reproduce mesoscale cyclones, such as polar lows (Stoll et al., 2021), and hence 280 the negligible importance of mesoscale eddies for the total energy transport appears reasonable. Due to its negligible role, we include the mesoscale into the synoptic transport for the remainder of this study.

4.2 Seasonal transport

Some transport patterns become more apparent when seasons are considered. The NH summer and the SH winter are here defined by the months June to August, and the NH winter and the SH summer by the months December to February. Due 285 to seasonal variations in the thermal contrast between the equator and poles, more energy is transported poleward in the winter than in the summer hemisphere (Fig. 5a,d) in good agreement with previous studies (e.g. Peixoto and Oort, 1992). The seasonality in the transport is larger in the NH than the SH, as also noted by Trenberth and Stepaniak (2003a). This is effected by a larger annual cycle in the temperature in the NH due to its large continents having a smaller heat capacity than the oceans

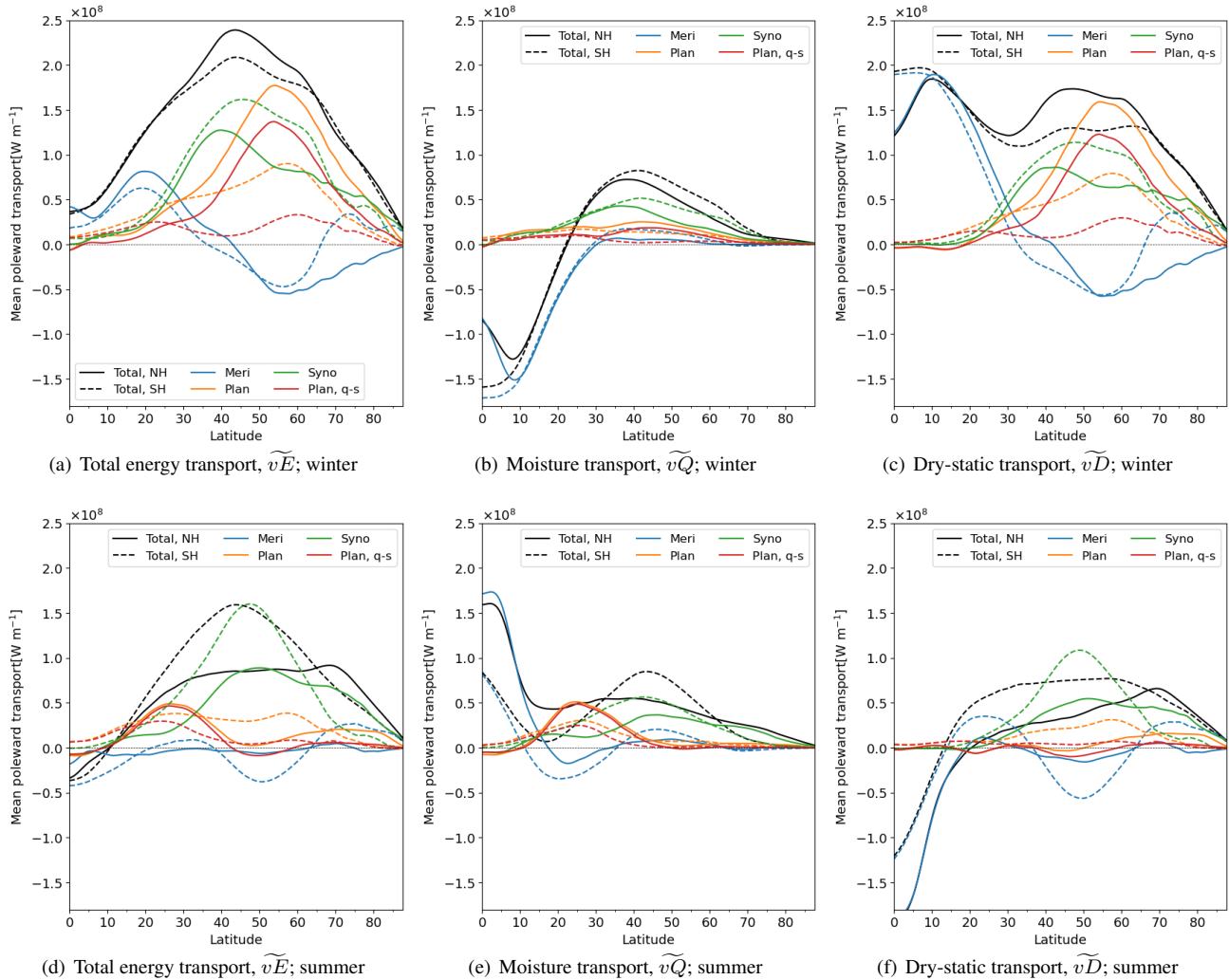


Figure 5. As Figure 4, but for the seasonal-mean transport of (a-c) winter, and (d-f) summer for (a,d) the total energy transport, (b,e) its latent component, and (c,f) its dry-static component.

in the SH. Still, the hemispheres share many characteristics in the atmospheric energy transport when it comes to seasonality.
 290 In spring and autumn the energy transport is in the main features similar to the annual-mean transport (Fig. 4, S7).

The zone separating northward and southward total transport is around 10° latitude in the summer hemisphere (Fig. 5d), the location of the intertropical convergence zone (ITCZ). In the tropics, the meridional overturning circulation, $\tilde{v}E_{meri}$, is most important (Fig. 5, blue). It transports energy from around ITCZ to the winter subtropics, whereas moisture, $\tilde{v}Q_{meri}$, is advected in the opposite direction.

295 In contrast to the planetary transport, $\tilde{v}E_{plan}$, the synoptic transport, $\tilde{v}E_{syno}$, is little influenced by seasonality, in broad agreement with transient transport in Trenberth and Stepaniak (2003a). In the extra-tropics of both hemispheres, the summer is



dominated by synoptic transport, \widetilde{vE}_{syno} . Differently, in winter both planetary and synoptic waves are highly relevant for the energy transport. In the NH winter, planetary waves, \widetilde{vE}_{plan} , contribute to more transport than do synoptic waves, mainly by its quasi-stationary component, $\widetilde{vE}_{plan}^{q-s}$. In the SH winter, planetary transport is also important, but mostly in a transient form, $\widetilde{vE}_{plan}^{tran}$, whereas its stationary part is small as noted previously (Oort and Peixóto, 1983).

In the subtropics of the summer hemisphere, quasi-stationary planetary waves, $\widetilde{vE}_{plan}^{q-s}$, are among the largest contributor to poleward energy transport (Fig. 5d). These waves are transporting energy mainly in the form of moisture, $\widetilde{vQ}_{plan}^{q-s}$ (Fig. 5e) and appear to represent the summer monsoon and long-lasting sub-tropical high-pressure systems.

4.3 Inter-annual variability

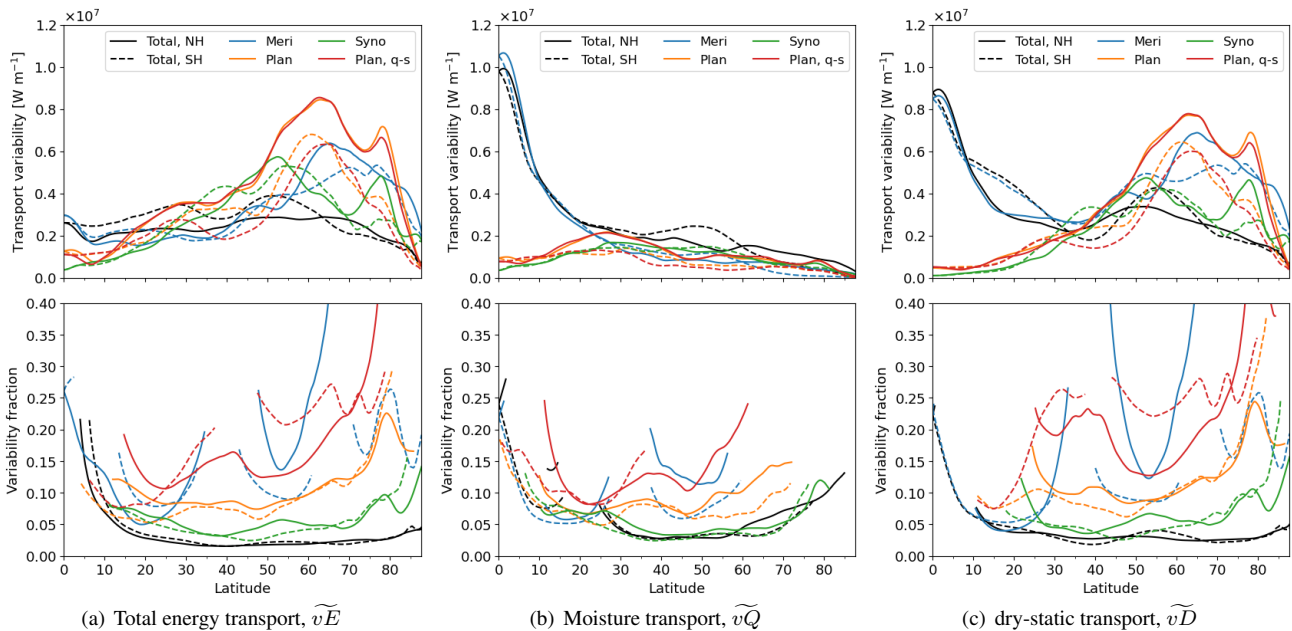


Figure 6. (a, upper panel) Inter-annual variability in the meridional energy transport, computed as the standard deviation in the annual transport, from ERA5 for the years 1979 - 2021 (black). The energy transport is divided into the meridional overturning circulation (blue) and wave components at the planetary (orange) and synoptic (green) scales. Solid and dashed lines depict the Northern and Southern Hemisphere, respectively. (Lower panel) The fraction of the variance of each transport component related to its absolute mean transport. Values are masked at latitudes $\pm 5^\circ$ where the mean transport crosses zero and where the absolute mean is smaller than 5% of the zonal-maximum of the total transport. (b) and (c) as (a) but for the latent and dry-static energy transport.

In this study, the inter-annual variability in the energy transport is computed by the standard deviation of the annual-mean transport. The total energy transport, \widetilde{vE} , is only varying by a few percent between years for all latitudes (Fig. 6a). However, the inter-annual variability in the individual components is up to three times larger than the variability in the total transport especially in the extra-tropics (Fig. 6a). Hence, large transport in one component is typically compensated by smaller transport



in another component, as also noted by Trenberth and Stepaniak (2003a) and Lembo et al. (2019). In contrast to the total
310 transport, the variability of the moisture transport components, \widetilde{vQ} , are rather summing up to the total variance (Fig. 6b). We
hypothesise that the different co-variability of the scale contributions for energy and moisture transport are due to different
mechanisms leading to energy and moisture transport as further explained in a subsequent study.

The tropics feature large inter-annual variability in the moisture transport, \widetilde{vQ} , and approximately equally large variability
in the dry-static transport, \widetilde{vD} , whereas the variability in total transport, \widetilde{vE} , is only a fifth of the moisture transport variability
315 (Fig. 6). This means that in the tropics, anomalous latent transport is typically compensated by opposed anomalies in the dry-
static transport. Hence, the Hadley circulation transports more latent energy in some years, although this has little effect on the
total energy transport.

In the extra-tropics, the planetary transport, \widetilde{vE}_{plan} , exhibits the largest inter-annual variability and varies by approximately
10% (Fig. 6), even though the annual-mean planetary transport is mainly smaller (Fig. 4) than the synoptic transport, \widetilde{vE}_{syno} ,
320 which varies by around 5%. The large planetary variability is mainly attributed to its quasi-stationary component, $\widetilde{vE}_{plan}^{q-s}$,
whereas its transient component, $\widetilde{vE}_{plan}^{tran}$, is much less variable (not shown). This demonstrates the "quasiness" of the quasi-
stationary transport, which is the transport component varying most from year to year. This appears to express the importance
of annual modes creating quasi-stationary planetary transport and changing states between years.

The extra-tropical moisture transport, \widetilde{vQ} , is varying approximately equally for planetary, \widetilde{vQ}_{plan} , and synoptic waves,
325 \widetilde{vQ}_{syno} (Fig. 6b). However, due to synoptic waves being responsible for most of the moisture transport in the extra-tropics
(Fig. 4b), the variability fraction is considerably higher for the planetary than the synoptic moisture transport.

5 Discussion and conclusion

In this study, we analyse the global atmospheric circulation by separating the meridional energy transport in the ERA5 re-
analysis by spatial scales, by moisture and dry-static components, and by quasi-stationary and transient parts. We apply a new
330 approach by using the wavelength instead of the wavenumber for separating the energy transport by scales for all latitudes. We
argue that a separation between planetary and synoptic eddies at a wavelength of 8,000 km and towards mesoscale eddies at
2,000 km capture our intuitive understanding of these waves as well as previously demonstrated differences between the scales.

A clear spatial separation between the synoptic and planetary scale may not exist, but a spatial decomposition has been
demonstrated to be useful for better understanding the atmospheric circulation and its impact on the local climate (Baggett and
335 Lee, 2015; Graversen and Burtu, 2016; Röthlisberger et al., 2019). Here, we provide further arguments for the usefulness of
the separating the energy transport by the spatial scale.

Different from the classical separation into quasi-stationary and transient energy transport, the transport is quite similar
in the spatial scales for both hemispheres, pointing towards the scale separation being a rather general method. This is most
obvious in the quasi-stationary transport, $\widetilde{vE}_{plan}^{q-s}$, which is mainly important in the NH extra-tropical winter, whereas planetary
340 transport is highly relevant in both hemispheres.



In the annual-mean, most energy and moisture in the extra-tropics is transported by synoptic eddies, \widetilde{vE}_{syno} . It is astonishing that despite all possible eddies, waves at scales in the rather narrow band between 2,000 and 8,000 km are responsible for the majority of the meridional energy transport for the whole extra-tropics. As baroclinic eddies lay within this band, this points towards the importance of baroclinic instability for inducing the extra-tropical energy transport as long being suspected (Holton and Hakim, 2013). However, other mechanism may contribute to the formation of eddies in this band. Hence, a future study is planned to investigate causes and effects of energy transport at different scales.

The synoptic energy transport reveals to be little influenced by the season. In contrast, extra-tropical planetary transport, \widetilde{vE}_{plan} is of major importance in winter mainly by transporting dry-static energy, \widetilde{vD}_{plan} , but less relevant in summer. In winter around the Arctic boundary, quasi-stationary planetary waves, $\widetilde{vE}_{plan}^{q-s}$, are dominating the energy transport. Such quasi-stationary planetary waves around the polar boundaries of both hemispheres feature the transport component with globally the largest inter-annual variability.

Also known characteristics of the atmospheric circulation are reproduced in this study, such as the dominance of the Hadley circulation in the tropics for transporting of energy, \widetilde{vE}_{meri} , to the winter hemisphere, and transporting of moisture, \widetilde{vQ}_{meri} in the opposite direction. In the subtropical summer, quasi-stationary planetary waves transporting moisture, $\widetilde{vQ}_{plan}^{q-s}$, are the largest contributor to poleward energy transport, which is associated with monsoon systems.

In this study, the atmospheric transport is analysed on an annual-mean and seasonal-mean basis, whereas individual weather events feature a large variety of transport patterns (Lembo et al., 2019). Some planetary transport events in the extra-tropics are for example equatorward. Hence, when the seasonal-mean planetary transport is close to zero, it means that poleward and equatorward transport events are balancing each other. The intra-seasonal distribution of the different transport components is investigated in a follow-up study. Further, a follow up study investigates how the energy transport in its components may change with global warming.

Data availability. The ERA-5 dataset is publicly available. The computed decomposition of the energy transport based on ERA-5 and the code for the analysis is willingly provided on request.

Competing interests. The authors declare no competing interests.

Acknowledgements. Thanks to ECMWF for providing access to data from the ERA5 reanalysis. The data were partly processed at the supercomputer FRAM and stored at NIRD, both provided by the Norwegian Research Infrastructure Services (NRIS) Sigma2 AS under the projects NN9348K and NS9063K, respectively.



References

- Ali, S. M., Martius, O., and Röthlisberger, M.: Recurrent Rossby wave packets modulate the persistence of dry and wet spells across the globe, *Geophys. Res. Lett.*, 48, e2020GL091452, 2021.
- 370 Baggett, C. and Lee, S.: Arctic warming induced by tropically forced tapping of available potential energy and the role of the planetary-scale waves, *Journal of the Atmospheric Sciences*, 72, 1562–1568, 2015.
- Bjerknes, J.: On the structure of moving cyclones, *Geophys. Publ.*, 1, 8 pp, 1919.
- Businger, S. and Reed, R. J.: Cyclogenesis in cold air masses, *Weather and Forecasting*, 4, 133–156, 1989.
- 375 Graversen, R. G.: Do changes in the midlatitude circulation have any impact on the Arctic surface air temperature trend?, *Journal of climate*, 19, 5422–5438, 2006.
- Graversen, R. G. and Burtu, M.: Arctic amplification enhanced by latent energy transport of atmospheric planetary waves, *Quarterly Journal of the Royal Meteorological Society*, 142, 2046–2054, 2016.
- Graversen, R. G., Stoll, P. J., and Rydsaa, J. H.: Hvorfor er Arktis det området i verden med raskest oppvarming?, *Naturen*, 145, 160–167, 380 2021.
- Hadley, G.: VI. Concerning the cause of the general trade-winds, *Philosophical Transactions of the Royal Society of London*, 39, 58–62, 1735.
- Heiskanen, T., Graversen, R. G., Rydsaa, J. H., and Isachsen, P. E.: Comparing wavelet and Fourier perspectives on the decomposition of meridional energy transport into synoptic and planetary components, *Quarterly Journal of the Royal Meteorological Society*, 146, 385 2717–2730, 2020.
- Hersbach, H., Bell, B., Berrisford, P., Hirahara, S., Horányi, A., Muñoz-Sabater, J., Nicolas, J., Peubey, C., Radu, R., Schepers, D., et al.: The ERA5 global reanalysis, *Quarterly Journal of the Royal Meteorological Society*, 146, 1999–2049, 2020.
- Hofsteenge, M. G., Graversen, R. G., Rydsaa, J. H., and Rey, Z.: The impact of atmospheric Rossby waves and cyclones on the Arctic sea ice variability, *Climate Dynamics*, <https://doi.org/doi.org/10.1007/s00382-022-06145-z>, 2022.
- 390 Holton, J. and Hakim, G.: *An Introduction to Dynamic Meteorology*, vol. 5, Academic Press, New York, USA, 2013.
- Lee, S., Woods, C., and Caballero, R.: Relation between Arctic moisture flux and tropical temperature biases in CMIP5 simulations and its fingerprint in RCP8.5 projections, *Geophysical Research Letters*, 46, 1088–1096, 2019.
- Lembo, V., Messori, G., Graversen, R., and Lucarini, V.: Spectral Decomposition and Extremes of Atmospheric Meridional Energy Transport in the Northern Hemisphere Midlatitudes, *Geophysical Research Letters*, 46, 7602–7613, 395 <https://doi.org/https://doi.org/10.1029/2019GL082105>, 2019.
- Lorenz, E.: The nature and theory of the general circulation of the atmosphere, *World meteorological organization*, 161, 1967.
- Oort, A. H. and Peixóto, J. P.: Global angular momentum and energy balance requirements from observations, in: *Advances in Geophysics*, vol. 25, pp. 355–490, Elsevier, 1983.
- Orlanski, I.: A rational subdivision of scales for atmospheric processes, *Bulletin of the American Meteorological Society*, pp. 527–530, 1975.
- 400 Papritz, L. and Dunn-Sigouin, E.: What configuration of the atmospheric circulation drives extreme net and total moisture transport into the Arctic, *Geophysical Research Letters*, 47, e2020GL089769, 2020.
- Peixoto, J. P. and Oort, A. H.: *Physics of climate*, American Institute of Physics, 1992.
- Priestley, M. D. K. and Catto, J. L.: Future changes in the extratropical storm tracks and cyclone intensity, wind speed, and structure, *Weather and Climate Dynamics*, 3, 337–360, <https://doi.org/10.5194/wcd-3-337-2022>, 2022.



- 405 Rossby, C.-G.: Relation between variations in the intensity of the zonal circulation of the atmosphere and the displacements of the semi-permanent centers of action, *J. mar. Res.*, 2, 38–55, 1939.
- Röthlisberger, M., Frossard, L., Bosart, L. F., Keyser, D., and Martius, O.: Recurrent synoptic-scale Rossby wave patterns and their effect on the persistence of cold and hot spells, *Journal of Climate*, 32, 3207–3226, 2019.
- Rydsaa, J. H., Graverson, R., Heiskanen, T. I. H., and Stoll, P.: Changes in atmospheric latent energy transport into the Arctic: Planetary
410 versus synoptic scales, *Quart. J. Roy. Meteorol. Soc.*, 2021.
- Shaw, T., Baldwin, M., Barnes, E. A., Caballero, R., Garfinkel, C., Hwang, Y.-T., Li, C., O’gorman, P., Rivière, G., Simpson, I., et al.: Storm track processes and the opposing influences of climate change, *Nature Geoscience*, 9, 656–664, 2016.
- Stoll, P. J., Spengler, T., Terpstra, A., and Graverson, R. G.: Polar lows – moist-baroclinic cyclones developing in four different vertical wind shear environments, *Weather and Climate Dynamics*, 2, 19–36, <https://doi.org/10.5194/wcd-2-19-2021>, 2021.
- 415 Trenberth, K. E.: Climate diagnostics from global analyses: Conservation of mass in ECMWF analyses, *Journal of Climate*, 4, 707–722, 1991.
- Trenberth, K. E. and Caron, J. M.: Estimates of meridional atmosphere and ocean heat transports, *Journal of Climate*, 14, 3433–3443, 2001.
- Trenberth, K. E. and Stepaniak, D. P.: Covariability of components of poleward atmospheric energy transports on seasonal and interannual timescales, *Journal of climate*, 16, 3691–3705, 2003a.
- 420 Trenberth, K. E. and Stepaniak, D. P.: Seamless poleward atmospheric energy transports and implications for the Hadley circulation, *Journal of Climate*, 16, 3706–3722, 2003b.
- Vallis, G. K.: *Atmospheric and oceanic fluid dynamics*, Cambridge University Press, 2017.
- Vihma, T., Graverson, R., Chen, L., Handorf, D., Skific, N., Francis, J. A., Tyrrell, N., Hall, R., Hanna, E., Uotila, P., et al.: Effects of the tropospheric large-scale circulation on European winter temperatures during the period of amplified Arctic warming, *Int. J. Climatol.*, 40,
425 509–529, 2020.